

THE PENNSYLVANIA STATE UNIVERSITY  
SCHREYER HONORS COLLEGE

DEPARTMENT OF BIOLOGY

Exploring the Effects of Inequities in Treatment Access on Resistance Emergence in  
*Caenorhabditis elegans*.

ANTON ALUQUIN  
SPRING 2023

A thesis  
submitted in partial fulfillment  
of the requirements  
for a baccalaureate degree  
in Immunology and Infectious Diseases  
with honors in Immunology and Infectious Diseases

Reviewed and approved\* by the following:

David Kennedy  
Assistant Professor of Biology  
Thesis Supervisor

Robert Paulson  
Professor of Veterinary and Biomedical Sciences  
Honors Advisor

\* Electronic approvals are on file.

## ABSTRACT

Antimicrobial resistance is a problem of increasing global concern. Access to proper treatments such as antimicrobial drugs and vaccines is one way by which we can mitigate the disease burden of these resistant infections. However, inequitable and patchwork treatment of these infections at the individual and population level may impose serious consequences for the severity of this growing problem. While there have been observational and epidemiological studies documenting the effects of differences in antimicrobial prescription rates as well as differences in antimicrobial resistant disease burden between advantaged and disadvantaged groups, experimental studies involving inequitable access on drug resistance have only been investigated through the lens of host jumps. Previous work in bacterial models has established evolving bacteriophages in mixed populations of susceptible and non-susceptible bacterial strains, resulting in the bacteriophage better infecting the non-susceptible hosts. While the effects of intermediate population ratios on host jump have been studied, the effects of intermediate population ratios on the resistance evolution dynamics of a pathogen to a therapeutic treatment have not been well documented. This thesis investigates the effects of intermediate population ratios on treatment resistance emergence in *Caenorhabditis elegans* and its recently discovered natural pathogen Orsay virus. Using a treatment that primes the RNA-interference response of *C. elegans*, various population ratios of RNAi-treated strains and non-RNAi-treated strains were mixed and infected with Orsay virus. This virus was passage through 10 sequential generations of worm populations. A modified Tissue Culture Infectious Dose 50 assay was then used to assess the 10<sup>th</sup> passage virus's relative resistance to the treatment. We hypothesize that intermediate ratios will lend to an increased emergence of treatment resistance in the virus

populations, due to the combined effects of maximum selection pressure with the maximum amount of available susceptible hosts. The results of this experiment present suggestive evidence to support this hypothesis, showing a suggestive significant increase in the model estimate average of the 20% group compared to the 0% and 100%. However, skewed omission of undefined TCID<sub>50</sub> measures, and the high variation of the data muddle the relationship that was expected. Continuing the experiment with more passages and documenting the other effects on the fitness of the virus will help further explore the work done here on the relationship between health inequities and antimicrobial resistance.

**TABLE OF CONTENTS**

LIST OF FIGURES .....	iii
LIST OF TABLES.....	iv
ACKNOWLEDGEMENTS.....	v
Chapter 1 Introduction .....	1
Chapter 2 Methods.....	6
Chapter 3.....	16
Chapter 4 Discussion .....	21

**LIST OF FIGURES**

Figure 1: Experimental Treatment Groups and Controls .....	9
Figure 2: Experimental Schematic for Evolution of Orsay Virus .....	11
Figure 3: Resistance Assay .....	14
Figure 4: qPCR Data from Experimental Treatment Groups with different ratios of % Treated. ....	17
Figure 5: TCID50 values for each evolutionary line with Treated (R) or Non-Treated (EV) treatment groups .....	18
Figure 6: Model estimate comparisons of "Proxy for Escape" for each %jyls group.....	20

## ACKNOWLEDGEMENTS

I would like to acknowledge the key role that the mentorship and help that David Kennedy and Amrita Bhattacharya both provided in guiding this process of this thesis. Dr. Kennedy was paramount in guiding me through the conceptual basis of this thesis, the planning of the experimental design, the analysis of the data, and revising and writing this thesis. Dr. Bhattacharya was essential in teaching me the benchtop techniques and skills of critical thinking that sparked the genesis of this experiment. Helena Laukitis and Dr. Bhattacharya were both immensely helpful in helping maintain lab supplies needed for this experiment and helping with various tasks such as labeling tubes and writing down numbers. I would like to acknowledge Huck Life Sciences, the Center for Infectious Disease Dynamics, and the Department of Biology for providing a space for me to pursue this question. I would also like to thank my professors, friends, and lab colleagues in supporting me every step of the way. Lastly, I want to thank my family and my parents for imparting a love for science that was the first step in the formulation of this thesis. Without them, this question would still be just a question.

## Chapter 1

### Introduction

Antimicrobial resistance—or the phenomenon in which microbes survive despite the use of antimicrobials that once killed them—is one of the largest emerging problems of today. Resistant pathogens impose a huge burden on the quality and duration of human life, with the CDC estimating that there are more than 2.8 million infections and 35,000 deaths per year that can be attributed to antibiotic resistance in the United States<sup>1</sup>. On a global scale, the World Health Organization has documented the need for action to combat the economic effects of increased incidence of disease, increased impact on the food supply chain, and losses in productivity due to sickness<sup>2</sup>. While calls to coordinate efforts to address antimicrobial resistance across global organizations and within countries have been strong, the slow-moving efforts of top-down approaches have hindered these efforts<sup>3</sup>.

In the same vein, public health efforts have also been slow to address health inequities in infectious diseases generally. These health inequities arise from social and systemic structures that result in differences in outcomes and susceptibilities, often leading to negative consequences for populations that are at most risk. For example, data from the Centers for Disease Control about the emergence of the SARS-CoV-2 pandemic indicate that African Americans and Hispanic Americans were—and still are—at a higher risk for getting COVID-19 and being hospitalized from it<sup>4</sup>. A higher prevalence of chronic and underlying conditions, a higher probability of exposure due to overrepresentation in front-line jobs, and other economic structures were the health inequities that were most at display during the beginning of the

pandemic. Health inequities in treatment access was also a contributing factor in the severity of the SARS-CoV-2 pandemic, and which worsened health outcomes were also seen in antibiotic access in childhood bacterial acute febrile illnesses<sup>5</sup> and anti-retroviral therapy for human immunodeficiency virus<sup>6</sup>. Inequities in access to these treatments have led to increased disease burden and human mortality in both of these instances. Thus, while some of the problems arising from health inequities are also seen in noncommunicable diseases, infectious diseases pose a unique ecological dilemma. Due to the communicable and indiscriminate nature of these pathogens, limits in treatment access may affect both advantaged and disadvantaged population. These potential effects on advantaged populations may not have been well characterized, and this study hopes to address one of these potential effects—disparities in access to treatment.

Various studies have investigated the potential effects of health inequities on antimicrobial resistance. Studies have documented differences in antimicrobial prescription among different socioeconomic groups<sup>7</sup>, different racial groups<sup>8</sup>, and different genders<sup>9</sup>. These studies found that marginalized groups tended to be prescribed less antibiotics than privileged groups. However, antimicrobial prescription rates are not a direct proxy of antimicrobial usage, thus these studies only demonstrate that there are differences between advantaged and disadvantaged groups in access to antibiotics, not whether such differences will drive resistance evolution. A study by Wurcel et al 2021 found that prescription rates of various antibiotics differed immensely in treating various skin and soft tissue infections. Higher prescription of clindamycin was found in Black patients, even though the recommended treatment for soft tissue and skin infections is cefazolin, suggesting that access to proper treatment in the United States may be limited by structural racism.<sup>10</sup> Likewise, Neves et al 2019 observed differences in rates of bacterial colonization and resistance as a function of socioeconomic status, and found that



children from lower/middle class were more likely to be colonized by methicillin-resistant *Staphylococcus aureus* than those from high income families and, surprisingly, from children categorized as from the slums<sup>11</sup>.

Overall, little is known about the effect that inequities in treatment access have on the emergence of antimicrobial resistance. Furthermore, the literature regarding the intersection of antimicrobial resistance and health inequities is sparse. Thus, the effects of inequitable access to antimicrobial treatments on the emergence of resistance have almost entirely been studied through modeling or observational studies, with a dearth of experimental studies. To determine causality, studies experimentally studying these dynamics in an animal model could yield novel insight.

In contrast, studies have investigated the effects of population heterogeneity on host jumps. The general of these experiments is that two host types are combined in various ratios in the presence of a pathogen that is only able to infect one of the two hosts initially. The pathogen is then passaged until it is either lost or gains the ability to infect the previously resistant host. Using this experimental structure, Chabas et. al 2018 found that when combining susceptible and non-susceptible strains of *E. coli* bacteria in different ratios, the intermediate ratios of the strains more often resulted in bacteriophages that had, on average, evolved to better infect the non-susceptible hosts over time<sup>12</sup>. Benmayor et al 2009 likewise found that intermediate ratios of susceptible and non-susceptible strains of *Pseudomonas fluorescens* more often yielded bacteriophages that had evolved the ability to infect the non-susceptible hosts over time, specifically in the 0.1% and 1% percentage of non-susceptible hosts<sup>13</sup>. Both papers justify that the higher likelihood of evolution to infect non-susceptible strains at intermediate ratios is due to the tradeoffs between selection pressure and the availability of susceptible hosts. Homogenous

populations of susceptible strains impose no selection pressure on the pathogen population to evolve resistance, since the pathogen is already able to infect the host population. Homogenous populations of non-susceptible strains impose a high selection pressure on the pathogen to evolve infectivity. But since selection can only act if variation is present, and since the pathogen has no hosts to infect, it cannot replicate to yield the necessary variation, even if mutation is unlikely. By accounting for the stochastic nature of pathogen emergence and resistance emergence, these studies show that the effects of mixed populations on the ability of a pathogen to jump to a typically non-susceptible host. The justification for host jumps in these studies may also apply to the case of antimicrobial resistance. If so, inequities in access to proper antimicrobial resistance may facilitate the emergence of antimicrobial resistance in human populations. Thus, my work builds on the logic of this previous work to determine whether the evolutionary dynamics that play out in the context of host jumps also play out in the context of antimicrobial resistance evolution.

To study these dynamics, we used *Caenorhabditis elegans* (*C. elegans*) strains and a naturally occurring *C. elegans* virus, Orsay virus<sup>14</sup>, to investigate these questions. *C. elegans* has an RNA-interference antiviral immune pathway that recognizes double-stranded RNA (dsRNA), including the dsRNA produced during the Orsay virus replication. Recognition of dsRNA initiates a cascade of proteins that result in the recognition and degradation through complementary small RNAs<sup>14</sup>. A bacterial strain developed by Kennedy and Bhattacharya triggers the RNA interference pathway (RNAi) of *C. elegans* to specifically target Orsay virus through the production of small RNAs. This protects against infection and disease. This was confirmed in prior work by Kennedy and Bhattacharya through experimental exposure of hosts and confirming a lack of virus production by qPCR. The developed RNAi-induced protection

was used to model antibiotic treatment. To generate heterogeneity in the host population, two strains were utilized: one that has a functional RNAi pathway and another that has its RNAi pathway knocked out and is unresponsive to the RNAi treatment. When fed RNAi bacteria, the RNAi responsive worms are functionally drug-treated hosts, while the RNAi non-responsive worms are functionally untreated hosts. These two strains were used and mixed in different ratios to model disparities in treatment access. After 10 rounds of viral passage, we then assessed the virus for resistance using a modified tissue culture infectious dose 50 assay (TCID<sub>50</sub>). When experimentally evolving the Orsay virus in populations with varying levels of access to treatment, we hypothesize that resistance would emerge more often in the intermediate ratios of worms (40/60, 60/40, 80/20, etc.) than in the extreme ends (0/100, 100/0).

## Chapter 2

### Methods

The effect of treatment access on resistance evolution was studied using two strains of *Caenorhabditis elegans*. ERT71 is a standard RNA interference-responsive strain that also expresses green fluorescent protein (GFP) when infected with virus. Jyls8/rde-1 (hereafter referred to as "jyls") is an RNAi-deficient strain of worm. Both strains were constructed through modification of N2 worms and gifted to the Kennedy lab. Each strain was retrieved from frozen stocks stored at -80°C. During the experiment, stocks of each strain were reared on virus-negative Nematode Growth Medium (NGM) plates with OP<sub>50</sub> *Escherichia coli* (*E. coli*) bacteria as a food source. Strains were passaged every 3-4 days to prevent starvation by transferring 5 adult worms from old NGM plates to new NGM plates.

Our various treatments were conducted on slightly modified NGM plates (NGM-IPTG) plates because RNAi treatment requires that worms are reared on Nematode Growth Medium (NGM) that contains ampicillin and Isopropyl β-D-1-thiogalactopyranoside (IPTG) in order to maintain the bacterial plasmid and act as a promoter, respectively. To make 100 of these plates, 3 g of sodium chloride, 2.5 g of peptone, and 17 g of agar were mixed with 975 ml distilled water, autoclaved at a 30-minute liquid cycle, and left to sit in a water bath at 50 °C for 1 hour. 1 M IPTG and 100 µg/ml Ampicillin were retrieved from -20 °C freezer and added to the media in 1000X concentrations (1 mL to 1L of media). 1 mL of 1M MgSO<sub>4</sub>, 1M CaCl<sub>2</sub>, and 5mg/ml cholesterol in EtOH were combined with 25 ml of 1M KPO<sub>4</sub> buffer in the media and mixed well using a magnetic stir bar at 400rpm for 3 minutes. 10 ml of liquid media was poured into each 60 mm petri plate and left on the benchtop covered for 3 days to dry.

NGM-IPTG plates were then spotted one of two different *E. coli* bacterial lawns: one bacterial lawn that possessed the RNAi treatment plasmid (39 plates “R”) and one bacterial lawn that had a plasmid without the RNAi treatment gene (7 plates “EV”). Colonies from an “R” or “EV” colony were transferred from a Luria-Bertani broth plate to approximately 10 ml of liquid Luria-Bertani broth mixed with 100  $\mu$ l ampicillin. These liquid cultures were incubated for approximately 24 hours at 37 C° in a shaking incubator set to 100 rpm. After incubation, all the treatment and control NGM-IPTG plates were spotted with 200  $\mu$ l of those bacteria cultures and left out to dry for approximately 24 hours.

At the start of each experimental passage round, both ERT71 and *jyIs* worms were bleach synchronized to standardize the life stage of the worms during the course of the experiment. To do this, NGM plates with a recently starved population of worms were washed with 1800  $\mu$ l of autoclaved water, pipetted up and down to dislodge the eggs from the media, and transferred to a 1.5 ml microcentrifuge tube. Tubes were centrifuged at 1300 x G for 1 minute and 700  $\mu$ l of the supernatant was removed, retaining the pellet of worms in approximately 700  $\mu$ l of liquid. 300  $\mu$ l of 2:1 bleach to NaOH in water was added and vortexed repeatedly. Once most of the worms had been cleared by the bleach—approximately 4-6 minutes—the tubes were centrifuged again at the same speed, supernatant was removed until there was 100  $\mu$ l left, and 900  $\mu$ l of autoclaved water was added. Care was taken not to disturb the egg pellets at the bottom of the microcentrifuge tubes. This process was repeated twice more to wash the bleach off the eggs. After the third rinse and centrifuge, 900  $\mu$ l of the supernatant was removed and the tube was vortexed. 50  $\mu$ l of the eggs were put on each of two unspotted NGM plates and inspected for eggs under the microscope. These plates were left on the benchtop overnight to grow to the L1 life stage.

L1 worms were transferred to OP50 spotted NGM by washing them off with 1800  $\mu$ l, centrifuging at 1000X for 1 minute and removing the supernatant until there was only approximately 100  $\mu$ l left. The 100  $\mu$ l was vortexed and transferred to a spotted plate. Following approximately 2 days of growth of both strains of worms to the L4 stage (on NGM with 200  $\mu$ l of *E. coli* strain OP50 in Luria-Bertani broth), different ratios of ERT71 to jyls worms were added to the spotted NGM-IPTG plates. 20 worms total consisting of 0%, 20%, 40%, 60%, 80%, and 100% ERT71 worms were picked and transferred (ex: 40% treatment consisted of 8 ERT71's and 12 jyls's). An EV plate was made for each ratio as well. Plates were numbered 1-42, with six replicate plates for each ratio and a seventh plate for an EV control. Since this EV plate should not induce RNAi responses, we would expect there to be unrestrained growth of virus, but no selection for resistance. Further controls included an ERT71-only plate with ancestral virus to confirm the effectiveness of the RNAi treatment, a jyls-only plate with

ancestral virus to compare the ancestral virus to the evolved lines, a virus-negative plate with 10 ERT71 worms and 10 jyls worms to ensure no contamination, and a worm-negative, virus-positive plate to set a threshold above which there is clear evidence of virus replication (See Figure 1).

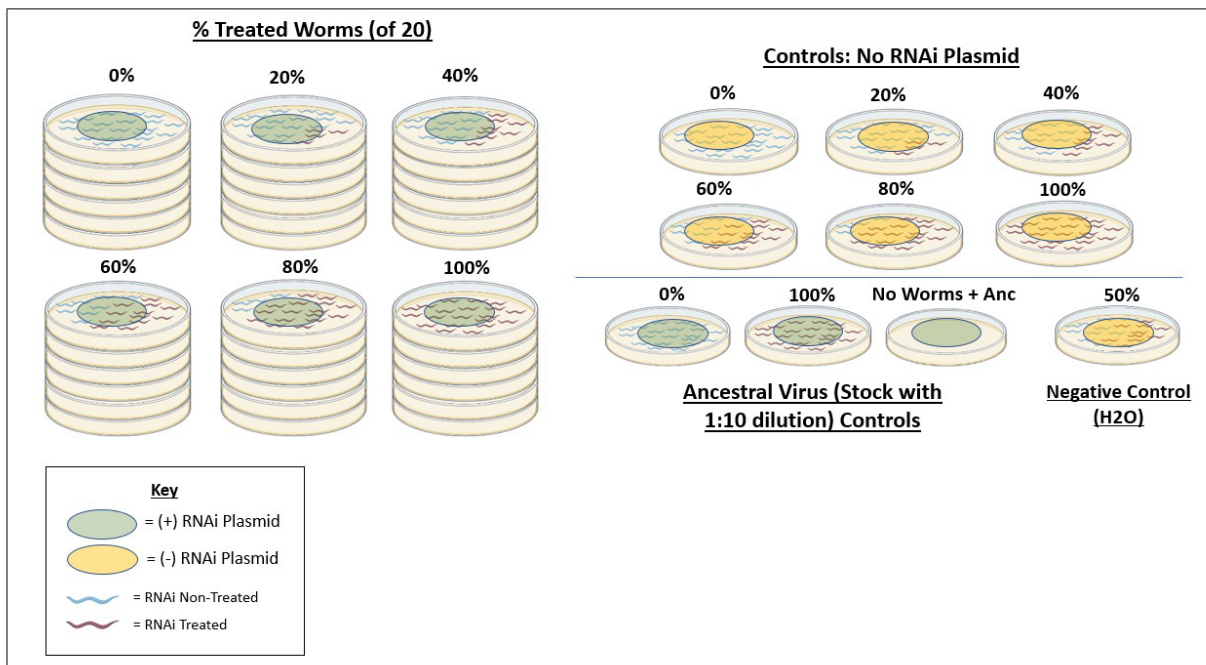


**Figure 1: Experimental Treatment Groups and Controls**

46 total RNAi-IPTG plates per passage round were used, 39 with RNAi plasmid-positive bacteria and 7 with RNAi plasmid-negative bacteria. RNAi Treated worms (ERT71) and RNAi non-treated worms (jyls) were added in treatments changing by 20% (0, 20, 40, 60, 80, 100). An RNAi-plasmid negative bacteria plate for each ratio was maintained to rule out the effects of passaging the virus over time on resistance. The 3 controls with ancestral stock virus were made new each passage, consisting of 100% treated, 100% non-treated, and a worm-negative control. A virus-negative control was also made every passage with an equal 50:50 ratio of hosts.

For the first passage replicate, 3  $\mu$ l of the stock Orsay virus was added to each plate immediately after worms were added except for the virus negative control. To collect virus, four days later, the worms were washed off the plate with 1800  $\mu$ l of autoclaved water. They were centrifuged at 1000 x G for 1 minute, had the supernatant removed, and washed with 900  $\mu$ l of autoclaved water. This was repeated twice more for a total of 3 washes. Then the supernatant was removed, 400  $\mu$ l of autoclaved water was added, and the worms were transferred to another tube with approximately 100  $\mu$ l of 0.5 mm silica beads and shaken in a TissueLyser II (Qiagen) for 2 minutes at a frequency of 30 shakes per second. Debris was removed with two centrifugation steps of 17 000 x G for 5 minutes each, where only the supernatant was retained, and the samples were stored at  $-80$  °C (see Figure 2).

For passages 2-10, the same experimental scheme was repeated, except the virus extracted from the previous passage was added to the corresponding treatment. For example, virus extracted from plate 22 was then added on to plate 22 for passage 2.

Samples were analyzed via quantitative polymerase chain reaction (qPCR) using an Orsay virus RNA probe, reverse primer, and forward primer, following standard lab protocol.



## Varying Population Ratios of Treatment Access on Resistance Emergence

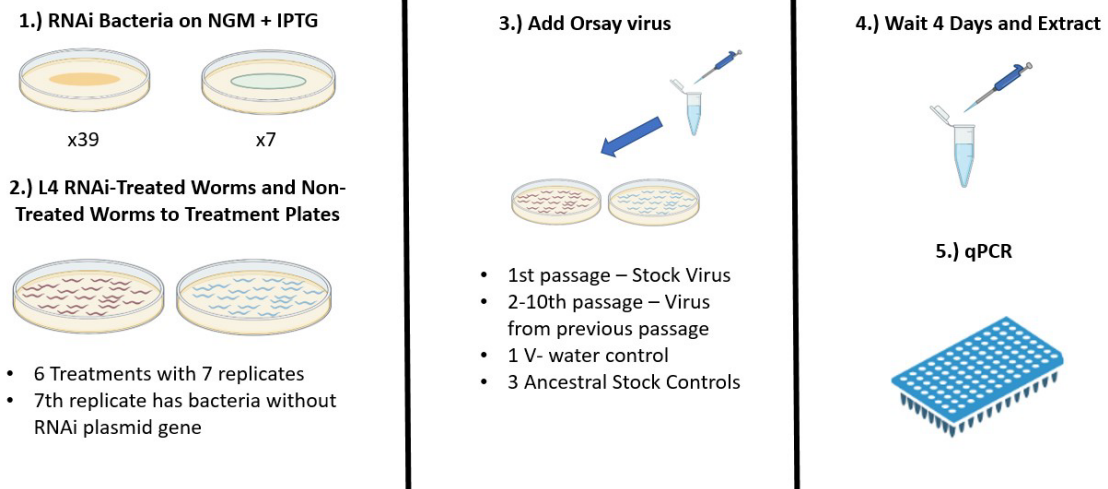


**Figure 2: Experimental Schematic for Evolution of Orsay Virus**

39 and 7 NGM-IPTG plates were spotted with R and EV bacteria, respectively. 6 R plates and 1 EV plate was made for each treatment and L4 worms were added in varying ratios. Immediately after, stock Orsay virus (for passage 1) or the previously extracted Orsay virus from the previous passage (for passages 2-10) was added. Ancestral stock controls documented the functioning of the RNAi treatment, any deficiencies in the JyLs worms, and the baseline viral load. 4 days passed and the virus was extracted from the worms and quantified using qPCR.

To assess the evolved Orsay virus strains for resistance to the RNAi treatment, a modified tissue culture infectious dose 50 (TCID<sub>50</sub>) assay was performed. TCID<sub>50</sub> refers to the amount of virus required to infect 50% of tissue culture samples (or in our case, the dose required to infect 50% of worm populations). TCID<sub>50</sub> assays determine the number of TCID<sub>50</sub> doses in a particular sample of virus. Somewhat confusingly, the amount of virus needed to infect an RNAi-treated or RNAi-non-treated host population likely differs, such that the same

tube of virus would have two different estimates for the number of TCID<sub>50</sub> doses. The proportional change in the number of TCID<sub>50</sub> doses in ERT71 worms that are either reared on R bacteria or EV bacteria through fluorescence from ERT71 worms is thus a measure of treatment efficacy. Changes in the ratio between these two measures (TCID<sub>50R</sub>/TCID<sub>50EV</sub>) can therefore be used as a measure of resistance. This approach was needed because there was no other way to normalize virus dose between treatments, since qPCR cannot distinguish between infectious and non-infectious viral RNA. A value of the ratio that is close to 1 indicates the evolved virus was able to infect equally well in the presence of the RNAi treatment or without the RNAi treatment, indicating the emergence of complete resistance to the treatment. A value of the ratio that is close to 0 indicates that the evolved virus was nearly fully inhibited by the RNAi treatment. The values for the TCID<sub>50</sub> studies were measured using the 10th passaged virus from each treatment.

The 10<sup>th</sup> passage virus for each evolutionary line was serially diluted in distilled water 4 times by a factor of 10. This generated dilution concentrations of 10<sup>-1</sup>, 10<sup>-2</sup>, 10<sup>-3</sup>, and 10<sup>-4</sup> relative to undiluted virus. In addition, the ancestral stock virus was diluted 4 times by a factor of 10, but the highest concentration of this was accidentally lower than for the other samples leading to dilution concentrations of 10<sup>-2</sup>, 10<sup>-3</sup>, 10<sup>-4</sup>, and 10<sup>-5</sup>.

24-well plates were filled with 2 ml of NGM: IPTG agar. Only the outside wells were used since the middle wells were not able to dry effectively. This minimized heterogeneity between wells. Thus, each plate had 16 usable wells. Each well was spotted with 10 µl of bacteria. 444 wells were spotted with R bacteria and 444 wells were spotted with EV bacteria.

44,000 ERT71 worms were needed to put 50 worms on 37 treatments with 4 serial dilutions for both an EV and R group each with 3 replicates (50 x 37 x 4 x 2 x 3 = 44,000). Thus, 100 plates of starved ERT71 worms grown on NGM with OP<sub>50</sub> were bleached and synchronized in a

modified version of the protocol that was used earlier in the experiment. Plates were washed with 1800  $\mu$ l of autoclaved water and pipetted into ten 15 ml Falcon tubes. These were centrifuged at 1300X for 3 minutes and the supernatant was removed until 7 ml remained. 3 ml of 2:1 bleach to NaOH in autoclaved water was added and observed until most of the worms disappeared. Tubes were centrifuged, supernatant was removed until there was 2 ml left. 8 ml of water was added and the process was repeated 3 times. After the final wash, supernatant was removed until 2 ml remained and 100  $\mu$ l was put on to 20 NGM plates for each of the 10 Falcon tubes. Plates were left at room temperature overnight. The L1 worms were then washed off with 1800  $\mu$ l of autoclaved water and put into multiple 15 ml Falcon tubes. Tubes were centrifuged at 1300X for 2 minutes and supernatant was removed until there was 2 ml remaining. Due to the high concentration of worms, three 1  $\mu$ l drops were put on to microscope slides and the average was taken. A volume of water that had an average concentration of 50 worms was added to each of the treatment wells.

Using the diluted virus mentioned earlier, 20  $\mu$ l of virus was then added to 24-well plates that contained wells with NGM-IPTG media, 50 ERT71 worms, and 10  $\mu$ l of either EV or R bacteria. These plates were made following the same methods as described above, except that each well contained 2 ml of agar rather than the 10 ml that go into the large 60 mm plates. These were left to dry for 72 hours before bacteria was spotted. Bacteria sat on the plates at room temperature for approximately 48 hours after which it was placed at 4 C for up to 7 days.

Each "treatment x dilution" combination of virus was used on 3 replicate wells. Evolutionary lines that did not make it to the end of the 10 passages were omitted from the TCID<sub>50</sub> assay.

The worms and virus were added on the same day. First, all the worms were added, then all of the viruses were added. Two days later the worms were observed under the SMZ18 microscope. The UV light was set to 50% brightness and the zoom magnification was set to 1.5x to standardize across wells. Note that because eyepieces are 10x, this gave a final magnification of 15X. Wells were examined by eye using a GFP filter. Green fluorescence indicates infection in ERT71 worms. The number of glowing worms was counted, but a threshold for glowing was set at 1 or more worms (see Figure 3), meaning that the detection of a single glowing worm was recorded as the presence of infection.

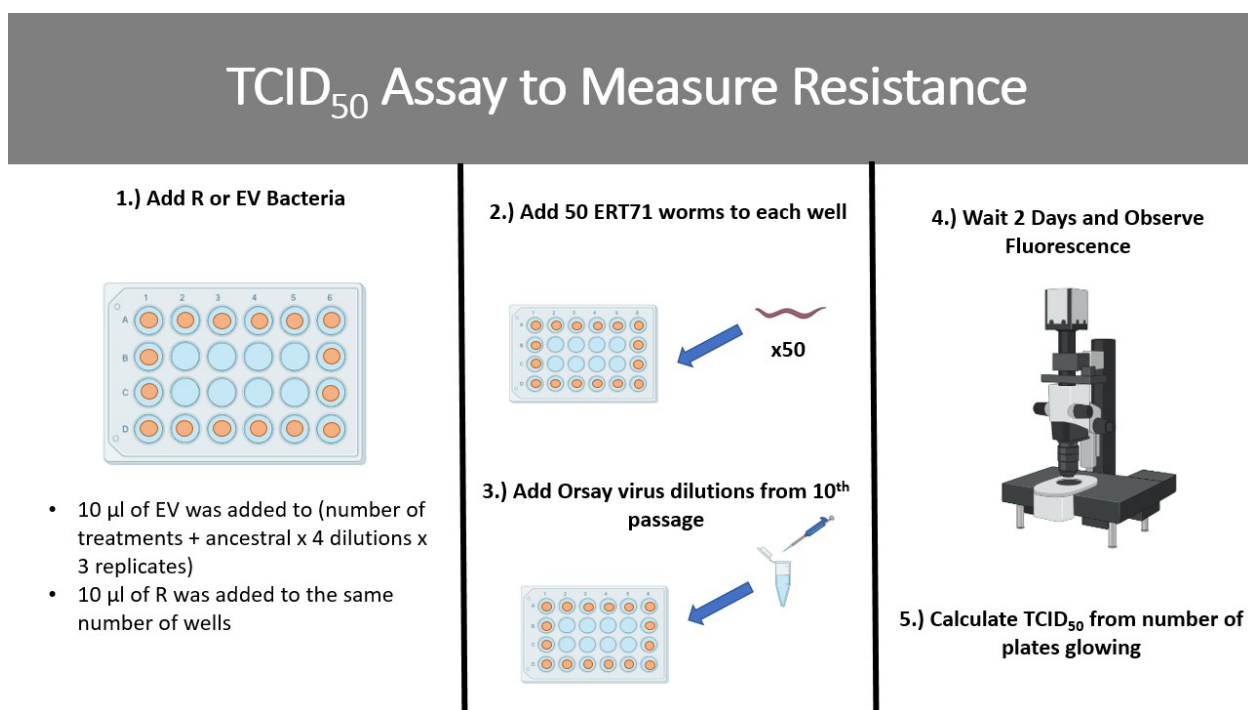


**Figure 3: Resistance Assay**

24-well plates with NGM-IPTG were spotted with EV or R bacteria. Only the outside of the plate was used to minimize heterogeneity. In this experiment, 888 wells were used. 50 worms were added to each well and each of the 4 dilutions for each treatment was added in 3 replicates. After two days, fluorescence was observed under the scope and TCID<sub>50</sub> was calculated in RStudio.

The number of wells that had glowing among the 3 replicates for each of the 4 serial dilutions was used to calculate the TCID<sub>50</sub> number for a particular treatment, resulting in an “EV” and “R” TCID<sub>50</sub> for each evolutionary line (TCID<sub>50EV</sub> and TCID<sub>50R</sub>). TCID<sub>50</sub> was calculated by D. Kennedy and based on a maximum likelihood approach using the approach from Shaw and Kennedy 2022<sup>15</sup>. The ratio of the maximum likelihood estimates TCID<sub>50R</sub> / TCID<sub>50EV</sub> yields a proxy for resistance to the RNAi treatment. All data analysis was performed in RStudio.

## Chapter 3

### Results

Quantitative PCR (qPCR) was performed after every evolutionary passage to monitor for the presence or absence of virus. For the evolutionary lines from the 0% treated (100% jyls and 0% ERT71 worms) to 80% treated groups (20% jyls and 80% ERT71 worms), the cycle threshold (Ct) means for each treatment over the ten passages was 13.91 for the 0%, 14.39 for the 20%, 14.6 for the 40%, 14.85 for the 60%, and 15.74 for the 80% taking into account 6 treatment lines. All 6 replicates that were attempted to passage in the 100% treated group (100% ERT71) showed undetectable virus after the second passage and were thus not passaged for the remainder of the experiment, apart from the EV control which persisted for all 10 passages. This was expected and indicates that resistance did not emerge for the 100% treated group (see Figure 4). The ancestral virus control with 100% ERT71 worms yielded a Ct value larger (ie. Less virus) than the 100% jyls worms with ancestral virus for passages 1-6, and 8, indicating the efficacy of the RNAi treatment. However, on passages 7, 9 and 10, the Ct of the 100% ERT71 group was comparable to that of the EV treatment groups, indicating that the treatment may not have been as effective in those instances.

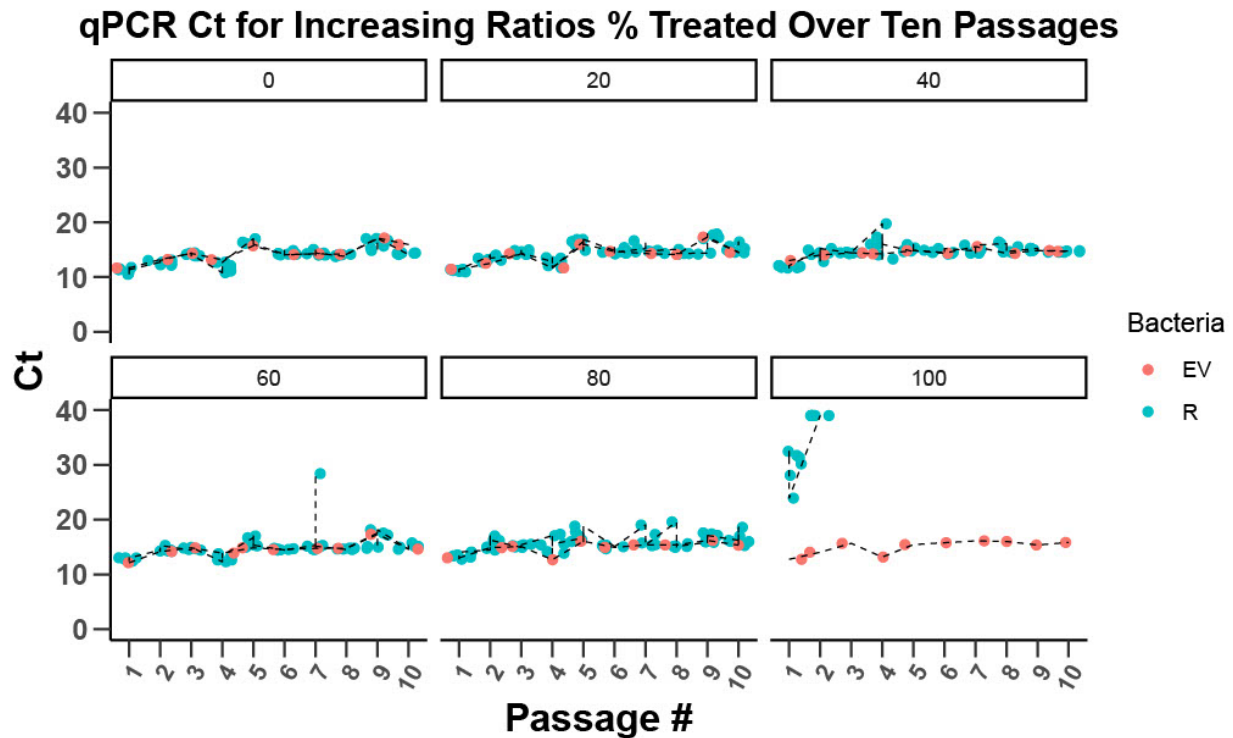


**Figure 4: qPCR Data from Experimental Treatment Groups with different ratios of % Treated.**

Treatment lines with EV are denoted in red and treatment lines with R are denoted in blue. Higher Cycle thresholds indicate less viral RNA is present in the worms at the end of the experimental passage. Virus was maintained in all the treatment groups over time, except for in 100% Treated group, where all R bacteria treatment lines were lost. A slight increase in Ct over the 10 evolutionary passages was observed, but the reason is unclear.

Glowing was seen consistently in the EV plates, especially from dilutions  $10^{-1}$  to  $10^{-4}$ . The mean number of glowing wells among all the EV treatments for 3 replicates was 2.97 for  $10^{-1}$ , 2.72 for  $10^{-2}$ , 1.75 for  $10^{-3}$ , and 0.17 for  $10^{-4}$ . Most of the  $10^{-1}$  and  $10^{-2}$  wells showed greater than 10 worms glowing. On the other hand, the R treatment wells rarely showed glowing. The average amount of plates glowing out of 3 for the various dilutions was 0.5 for  $10^{-1}$ , 0.14 for  $10^{-2}$ ,

0.08 for  $10^{-3}$ , and 0.03 for  $10^{-4}$ . Many of these wells only had 1 worm glowing. Many of the R treatments showed no glowing at any dilution, meaning a  $TCID_{50}$  threshold was not able to be calculated. Due to this, the threshold for glowing was set at 1 worm.

$TCID_{50}$  assay results for R and EV treatment are shown in Figure 5. A  $TCID_{50}$  of 1 indicates that there was no glowing found in any of the wells for any of the serial dilution groups ( $10^{-1}$  to  $10^{-4}$ ). 14 R lines had no glowing in any wells, with more lines from the lower % JyLs groups being dropped than in the higher % jyls groups. As the % of jyls worms increases, the  $TCID_{50}$  increases in both the EV and the R groups.

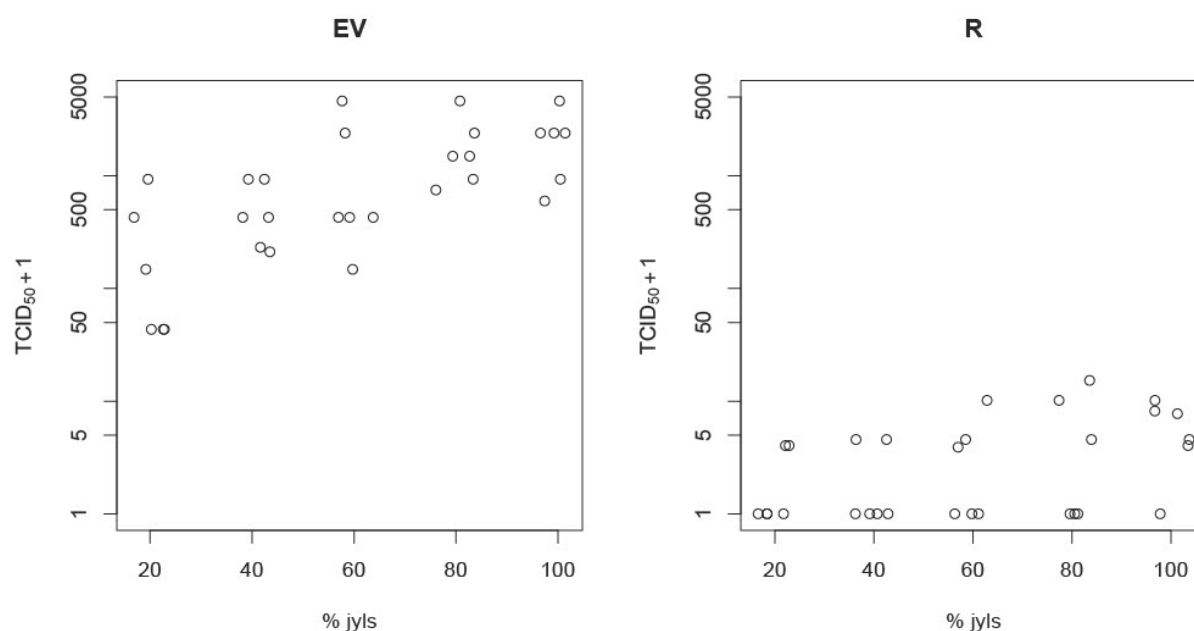


**Figure 5:  $TCID_{50}$  values for each evolutionary line with Treated (R) or Non-Treated (EV) treatment groups.**

The number of tissue culture infectious dose 50 ( $TCID_{50}$ s) plotted against %jyls. “% jyls” worms is equivalent in our experiment to the percent of the population without treatment. Each evolutionary line has both a  $TCID_{50EV}$  and a  $TCID_{50R}$ , though for many lines, none of the R wells showed glowing. These



points are plotted at 1 on the y-axis. A positive correlation between  $TCID_{50EV}$  and % jyls can probably be attributed to the differences in available jyls worms for virus to replicate in.

The resistance ratios comparing the  $TCID_{50R}/TCID_{50EV}$  were calculated and plotted (Figure 6). The model estimate was then obtained for each “%jyls” group, and any resistance ratio with a zero or undetermined value was omitted from the analysis. More values were omitted from the higher “%jyls” groups (i.e., 20% jyls only had 2 values while 100% had 5), mostly due to the constraints of the serial dilution range that was used in this experiment. Omitted points most likely had low  $TCID_{50}$  values, and a dilution of  $10^{-1}$  was too dilute to allow for infection and thus, glowing. The 20% treatment group was suggestively significantly higher in the group’s model estimate ability to escape the treatment (Likelihood ratio test,  $X^2 = 8.7$ ,  $df = 4$ ,  $p = 0.07$ ) . However, the variance of the two data points in this group is high, while also being less robust due to the omission of 4 data points.

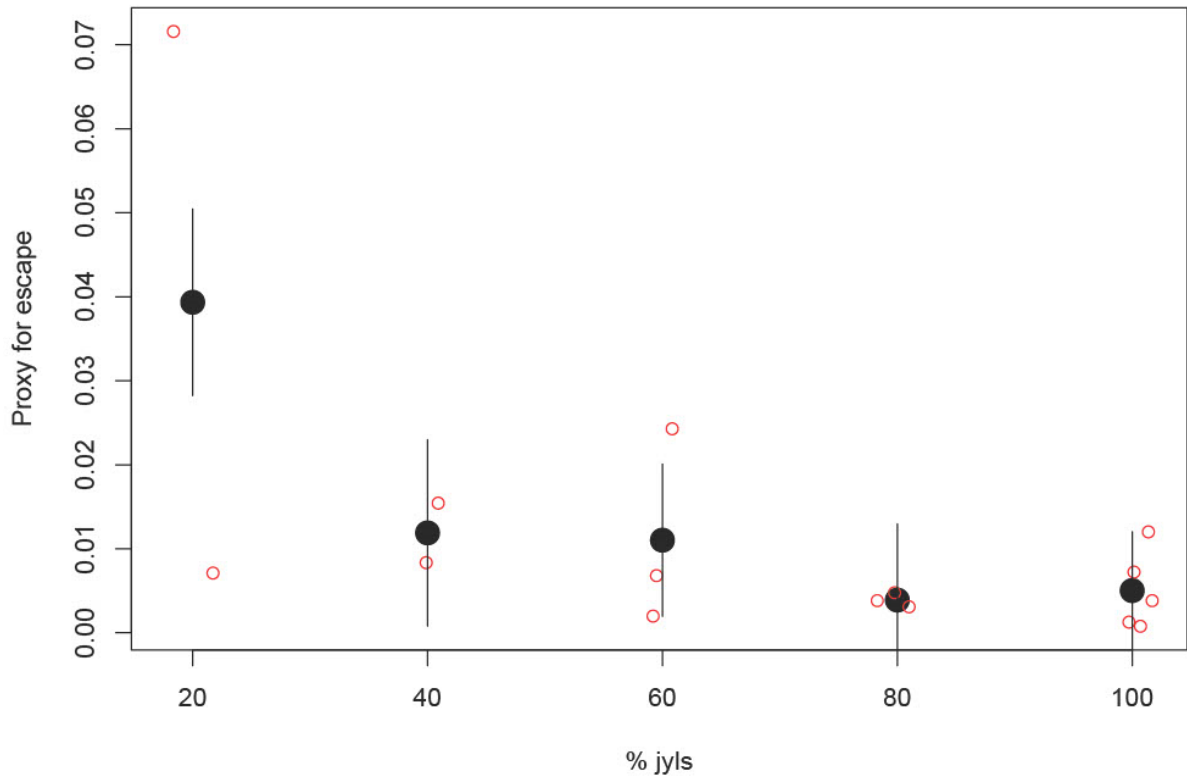


**Figure 6: Model estimate comparisons of “Proxy for Escape” for each %jyls group.**

Model estimate is an estimate of the true average of the data points. Proxy for escape is  $TCID_{50R}/TCID_{50EV}$  with any undetermined ratios being dropped from the dataset. More values were undetermined in the 20% jyls than the 100% jyls group, indicating the difference in dose and serial dilution window. There is a statistically significant difference in the proxy for escape in the 20% jyls treated group.

## Chapter 4

### Discussion

This thesis explores the effects of inequities in access to treatment on the emergence of treatment resistance. A serial passage experiment was conducted where the ratio of the population that was treated (RNAi-responsive strain of *C. elegans*) to the population that was not treated (RNAi-responsive strain of *C. elegans*) was varied in intervals of 20%, and after 10 passages resistance was characterized through a modified TCID<sub>50</sub> assay.

Health inequities are widespread, but action is slow because it relies on top-down action. Here, this work explores whether health inequities have negative consequences, not just for the disadvantaged population, but also for the privileged population. Previous work in bacteriophages showed that mixing two different hosts in intermediate ratios more often propagated the jump of the bacteriophage from the susceptible host to the non-susceptible host. Here we tested whether those same factors drove resistance. Suggestive evidence was found that intermediate ratios of treated hosts: non-treated hosts yielded resistance more often, as the 20% untreated group had a significantly higher model estimate mean than other groups. This supports our hypothesis, and parallels results in host range studies, demonstrating that even privileged individuals could benefit from reducing inequities in access to proper treatment.

Antimicrobial resistance—due to its existence in communicable pathogens—may also be exacerbated by the same differences in health outcomes between advantaged and disadvantaged populations. Lower- and middle-income countries and people of lower socioeconomic status may not have consistent access to newer antimicrobials, preventive measures, or healthcare providers that are effective against treating multi-drug resistant or extensively drug resistant pathogens<sup>16</sup>. This may worsen the spread of resistance and thus worsen both the disease burden on the

population but also the disease spread of these pathogens: for example, acute bacterial febrile illnesses such as pneumonias. One model saw that the elimination of resistance may reduce the burden of neonatal sepsis deaths due to resistant pathogens in 5 countries by 139,100 to 318,400 deaths over time<sup>16</sup>. The suspected disease burden of resistance has massive implications for human life and thus necessitates the need for exploration into the causative mechanisms of resistance.

The qPCR data shows a consistent presence of virus over the 10 passages in nearly all the evolved virus lines, except for treatments with 100% treatment-responsive worms where virus was lost from the experiment after the 2<sup>nd</sup> passage. Virus was lost in these 100% treatment groups presumably due to effective inhibition of replication from the RNAi treatment. Qualitatively, there seems to be only slight differences between the range of values for the 80% treated group and the 0% treated group, indicating that the virus was able to effectively replicate in the 20% jyls despite the lower amount of available non-treated hosts. The highest average Ct being in the 100% treatment group does not provide any evidence for resistance. No obvious differences in qPCR between the 1<sup>st</sup> and 10<sup>th</sup> passage for any EV treatments were seen, suggesting that any changes in Ct are unlikely to be due to the passage of the virus over time. Since the negative control confirming the function of the RNAi treatment was faulty in the last 3 passages of the evolution experiment, this may have resulted in the loss of any resistance mutations with a fitness cost, due to the absence of selection pressure. This may have led to a depression in the observed resistance estimates and a skewed representation of the true resistance levels.

The concentration of virus in the collected 10<sup>th</sup> passage samples also played a role in the resistance index, despite our best efforts in designing the resistance assay. This is because even

though we used 4 serial dilutions to encompass a wide range of viral concentrations, many “R” groups showed no glowing, yielding no defined TCID<sub>50R</sub> and thus no value for the resistance index. Omitting these points poses a problem; our data may show a significant relationship even if there is no true relationship. A smaller pool of TCID<sub>50</sub> values cannot rule out randomness as an explanation for the relationship seen in the data and may overestimate the model estimate mean for the resistance of a %jyls group. On the other hand, omission is important in controlling for the varying viral load at which each treatment sample was administered in the resistance assay. Since there was most likely a larger amount of virus extracted from the 100% jyls worm treatments, the threshold at which the TCID<sub>50</sub>'s would be captured by the experiment was more likely. Since the omitted TCID<sub>50</sub>'s are most likely nonzero, imposing a 0 is a misrepresentation of the true data. Assigning 0's to all points with undetermined values of TCID<sub>50</sub> imposes an artificial decrease on the model estimate mean that makes the value less encompassing of the true value. So, while omitting the undetermined TCID<sub>50</sub> values may show significance despite a small dataset, it better takes into account the problem of variation in viral load and better represents the data despite the constraints of the experimental design.

Despite the challenges with data analysis, the data show suggestive evidence for increased emergence of resistance in populations with intermediate ratios of treated and non-treated hosts. While the 100% treated/0% untreated samples had no lines that persisted, the ancestral stock virus could be used in a future experiment as a comparison to act as a 100% treated control which could work to support the evolution of resistance due to the experiment rather than due to variation in the virus itself. I attempted to do so, but accidentally used a 10-fold lower dose of ancestral virus than passage virus. As a result, none of the RNAi treated wells glowed in our resistance assay, and so as explained above, we were unable to use that data.

Further confirmatory work will also necessitate repeating the last 3 passages of the evolution experiment with a functional RNAi treatment, especially since the 100% ERT71 control had no virus inhibition. Furthermore, it would be useful to repeat the resistance assay to include a wider variety of serial dilution ranges (expanding perhaps to a 1:5 dilution as the most concentrated and  $1:1 \times 10^6$  as the least concentrated dilution) in addition to the ancestral virus. While there are caveats in the findings of this study, ranging from skewed omission of TCID<sub>50</sub> ratios to a lack of 100% treated virus control, certain samples had a biologically important two-fold to seven-fold increase in the ability for the evolved virus to escape the RNAi treatment. In the context of antimicrobial resistant pathogens, this may be sufficient to allow colonization of the pathogen in treated hosts and transmission through a population with varying levels of treatment responsiveness.

To further confirm the presence of resistance in the Orsay virus population, more evolutionary passages up to 15 or 20 generations of worms could be performed in order to see if more time increases the likelihood of emergence. Furthermore, or genomic analyses could be performed. More passages would allow for more time under selection pressure potentially clarifying the suggestive pattern we see in these samples, and a genomic analysis looking at various single nuclear polymorphisms between virus lines and the ancestral virus could highlight important resistance genes in the Orsay virus genome. Once several resistant viral strains are established, future work looking at evolution in varying ratios of worm populations and its effects on virulence, fecundity, and motility in *C. elegans* may also pose interesting questions. Some work has been done looking at the effects of intermediate populations on virulence evolution of various pathogen systems such as *Arabidopsis thaliana* and Turnip mosaic virus, where they found that intermediate populations affected the virulence of an evolved virus. The

evolutionary and ecological dynamics at play between virulence and resistance may propose further questions and answers at the heart of the problem of tackling resistance.

This study attempts to address the problem of antimicrobial resistance, specifically working to understand the complex factors that lead to the emergence of resistance in populations. Variation in hosts, interhost interactions, and therapeutic treatments all affect one another, and no model can perfectly encapsulate the stochastic nature of these complex interactions. However, the *C. elegans* model poses a unique way of investigating the effects of access to treatment on the emergence of virus resistance.

The work here has future implications for the importance in addressing healthcare access and antimicrobial resistance as compounding issues. The work in this thesis suggests that if access to prophylactic or therapeutic treatments is patchwork and uncoordinated, it may increase the chance of resistance emergence and potentially increase the disease burden. Thus, policies such as guaranteeing access to treatment through proper administration by pharmacies and healthcare providers, coordinated plans for treatment between countries to standardize care, ensuring the quality of these drugs, and addressing the social determinants of health are all paramount in addressing the problems of antimicrobial resistance and health inequities<sup>17</sup>. Policymakers and leaders may be informed by this research to justify the coordinated effort at the local, national, and global level to provide access to a greater amount of people of all different sociodemographic backgrounds. Likewise, as inequities in healthcare access may undermine the availability of effective treatment even for members of the privileged group. As resistance continues to pose a danger to people of all backgrounds, establishing the role that health inequities play on the emergence of resistance and the policies that are effective in addressing both is critical.

**BIBLIOGRAPHY**

1. Centers for Disease Control and Prevention. *Antibiotic resistance threats in the United States, 2019*. CDC <http://dx.doi.org/10.15620/cdc:82532>. (2019) doi:10.15620/cdc:82532.
2. World Health Organization. *Global action plan on antimicrobial resistance*. World Health Organization (2017).
3. O’Neill, J. *Tackling Drug-Resistance Infections Globally: Final Report and Recommendations. The review on Antimicrobial Resistance Chaired by Jim O’Neill*. [Online .... [https://amr-review.org/sites/default/files/160518\\_Final paper\\_with cover.pdf](https://amr-review.org/sites/default/files/160518_Final_paper_with_cover.pdf) (2016).
4. Romano, S. D. *et al. Trends in Racial and Ethnic Disparities in COVID-19 Hospitalizations, by Region — United States, March–December 2020*. *MMWR. Morbidity and Mortality Weekly Report* vol. 70 <https://www.cdc.gov/mmwr/volumes/70/wr/mm7015e2.htm> (2021).
5. Laxminarayan, R. *et al. Access to effective antimicrobials: a worldwide challenge*. *Lancet* **387**, 168–175 (2016).
6. Joint United Nations Programme on HIV/AIDS (UNAIDS). *DANGEROUS INEQUALITIES WORLD AIDS DAY REPORT | 2022*. <http://www.wipo.int/amc/en/mediation/rules> (2022).
7. Masiero, G., Filippini, M., Ferech, M. & Goossens, H. Socioeconomic determinants of outpatient antibiotic use in Europe. *Int. J. Public Health* **55**, 469–478 (2010).
8. Olesen, S. W. & Grad, Y. H. Racial/ethnic disparities in antimicrobial drug use, United States, 2014–2015. *Emerging Infectious Diseases* vol. 24 2126–2128 (2018).



9. Schröder, W. *et al.* Gender differences in antibiotic prescribing in the community: A systematic review and meta-analysis. *J. Antimicrob. Chemother.* **71**, 1800–1806 (2016).
10. Wurcel, A. G. *et al.* Variation by Race in Antibiotics Prescribed for Hospitalized Patients with Skin and Soft Tissue Infections. *JAMA Netw. Open* **4**, (2021).
11. Neves, F. P. G. *et al.* Differences in gram-positive bacterial colonization and antimicrobial resistance among children in a high income inequality setting. *BMC Infect. Dis.* **19**, (2019).
12. Chabas, H. *et al.* Evolutionary emergence of infectious diseases in heterogeneous host populations. *PLoS Biol.* **16**, e2006738 (2018).
13. Benmayor, R., Hodgson, D. J., Perron, G. G. & Buckling, A. Host Mixing and Disease Emergence. *Curr. Biol.* **19**, 764–767 (2009).
14. Félix, M. A. & Wang, D. Natural Viruses of Caenorhabditis Nematodes. *Annu. Rev. Genet.* **53**, 313–326 (2019).
15. Shaw, C. L. & Kennedy, D. A. Developing an empirical model for spillover and emergence: Orsay virus host range in Caenorhabditis. *Proc. R. Soc. B Biol. Sci.* **289**, (2022).
16. Mendelson, M. *et al.* Maximising access to achieve appropriate human antimicrobial use in low-income and middle-income countries. *Lancet* **387**, 188–198 (2016).
17. Evans, D. R., Higgins, C. R., Laing, S. K., Awor, P. & Ozawa, S. Poor-quality antimalarials further health inequities in Uganda. *Health Policy Plan.* **34**, III36–III47 (2019).

## ACADEMIC VITA

**Anton A. Aluquin**

### EDUCATION

B.S. in Immunology and Infectious Disease - Schreyer Honors College—2019 - 2023 (expected) The Pennsylvania State University, University Park, PA

- Minor in Health Policy and Administration,

### RESEARCH AND PUBLICATIONS

**Research Assistant, Dr. David Kennedy, Penn State University— February 2020 – Present**

- Investigating the role of inequities in access to treatment on drug resistance modeled in the *C. elegans* worm model organism
- Spearheaded gathering the data in a project investigating the relationship between antimicrobial resistance and characteristics of 57 clinically relevant bacterial pathogens.
  1. **(Under Review)** A. Bhattacharya, **A. Aluquin**, D. A. Kennedy . Exceptions to the rule: Why does resistance evolution not undermine antibiotic therapy in all bacterial infections?

### INTERNSHIPS

**American Public Health Association – Alliance for Disease Prevention & Response – June 2022 – August 2022**

- Aided in planning a coalition meeting to advocate for public health at the state and federal level
- Analyzed several leading Public Health Reports to build recommendations for public health infrastructure prioritization
- Facilitated partnership between several state public health associations and state organizations

## **EXTRACURRICULAR ACTIVITIES**

### **Field Organizer Lead for Central PA United – March 2021 – Present**

- Spearheaded the voter outreach strategies for the 2022 gubernatorial race
- Mobilized voter outreach by harnessing the power of conversations and human connection through door knocking and phonebanking

### **Presidential Leadership Academy – Summer 2020 – Present**

- Selected as one of 30 sophomores to engage in leadership development and critical thinking about political issues with classes taught by the President of the University

## **COMMUNITY SERVICE**

### **3/20 Coalition Structural Reform Chair (August 2021 – Present)**

- Advocated for police reform within local government systems by pushing for a community oversight Board and transparency surrounding use of force policies
- Mobilized antiracism campaign to call for antiracist reform in State College, PA

## **WORK EXPERIENCE**

- **Research Assistant in David Kennedy's Lab (May 2021 – Present)**
- **Research Assistant in Selena Ortiz's Lab (May 2021 – Present)**